Progress In Electromagnetics Research B, Vol. 7, 245–255, 2008

WAVEGUIDE AS A NEAR-FIELD MEASURING PROBE OF THE TWO-ELEMENT ARRAY RADIATOR

S. Paramesha

Department of E & C
AIT, Chikmagalur- 577102, Karnataka, India

A. Chakrabarty

Department of E & ECE
IIT, Kharagpur-721302, West Bengal, India

Abstract—In the analysis, an open-ended rectangular waveguide in an infinite ground plane is used as a near-field probe and the two-element waveguide array in an infinite ground plane is used as a radiator. Moment method analysis is used to find the reflection coefficient of the array element and probe voltage. The reflection coefficient of the array element, which is also an open-end of a rectangular waveguide, is computed and compared with the reflection coefficients, when the probe is at different positions in the near-field. The computations have also been carried out to find the induced probe voltage, when the probe scan in transverse plane (planar scanning) at a distance z_1 from the radiator. Good agreement is obtained between measured and MOM results.

1. INTRODUCTION

The radiating waveguide is a fundamental electromagnetic structure, and one about which a great deal is known. With the realization of large-scale microwave arrays, the subject of waveguide radiation and mutual coupling has aroused renewed interest. The waveguide elements in two-element array in an infinite ground plane being used as radiating elements are assumed to be excited in the dominant TE_{10} mode. An electromagnetic wave incident on the open-end of a waveguide being used as a near-field probe causes an electric field to be induced at the plane of the waveguide. The boundary conditions imposed at the radiating apertures and probe aperture by automatically taking

multiple reflections between radiator and probe, and also mutual coupling effect between radiating elements into account.

The field is described as a sum of M number of weighted sinusoidal basis functions, defined over the extent of the aperture at the plane of the waveguide. This field can be considered to be a magnetic current source which scattered some field into the free space and some field is scattered within the waveguide. The tangential components of the scattered magnetic field within the waveguide and that scattered into the free space must be continuous at the plane of the aperture. Enforcement of this boundary condition leads to an integral equation involving the M unknowns used to describe the aperture electric field. This is transformed into a matrix equation by taking moments with entire domain sinusoidal weighting functions [1]. A solution of this matrix equation provides the values of the unknown coefficients. The fields scattered inside and outside the waveguide are obtained in terms of these coefficients. Assuming a matched detector, the power received by the detector and the voltage measured by the measuring device are calculated.

2. FORMULATION OF THE PROBLEM

The geometry of the problem is a measuring waveguide probe at the near-field of a two-element waveguide array radiator and it is shown in Figure 1. The aperture dimension of each waveguide is $2a \times 2b$.

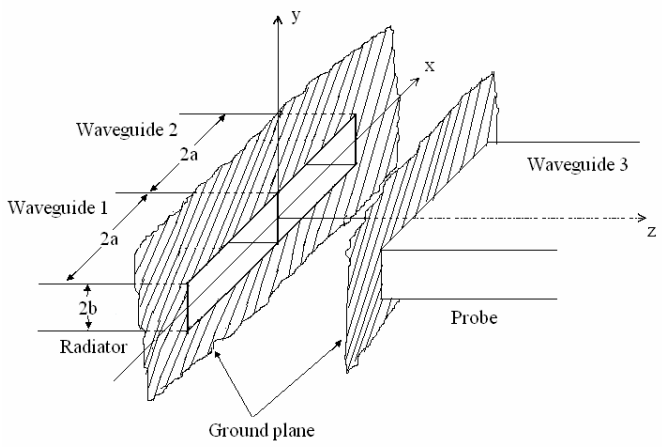

Figure 1. Open-ended waveguide as a near-field probe of the two-element array radiator.

The incident magnetic fields at the radiating waveguide apertures 1 and 2 for the dominant TE_{10} mode are given by:

$$H_x^{inc1} = -Y_0 \cos\left(\frac{\pi x}{2a}\right) e^{-j\beta z} \tag{1}$$

$$H_x^{inc2} = -Y_0 \cos\left(\frac{\pi x}{2a}\right) e^{-j\beta z} = H_x^{inc1} \tag{2}$$

and the electric fields at the radiating apertures 1 and 2 are described by:

$$\overrightarrow{E^1}(x', y', 0) = \widehat{u}_y \sum\nolimits_{p=1}^{M} E_p^1 e_p^1 \tag{3}$$

$$\overrightarrow{E^2}(x', y', 0) = \widehat{u}_y \sum\nolimits_{p=1}^{M} E_p^2 e_p^2 \tag{4}$$

where the entire domain basis functions e_p ($p = 1, 2, \ldots, M$) are defined by

$$e_p^1 = \begin{cases} \sin\left\{\dfrac{p\pi}{2a}(x+a)\right\} & \begin{cases} -a \le x \le a \\ -b \le y \le b \end{cases} \\ 0 & \text{elsewhere} \end{cases}$$
$$= e_p^2 \tag{5}$$

The equivalent magnetic current at aperture 1 for computing the externally radiated magnetic field using the plane-wave spectrum approach is given by [2]:

$$\overrightarrow{M_e^1} = 2\overrightarrow{E^1}(x', y', 0) \times \widehat{u}_z$$
$$= \widehat{u}_x \sum\nolimits_{p=1}^{M} 2E_p^1 \sin\left\{\frac{p\pi}{2a}(x+a)\right\} \begin{cases} -a \le x \le a \\ -b \le y \le b \end{cases} \tag{6}$$

The electric vector potential $\overrightarrow{F^1}$ at any point in space due to magnetic current at aperture 1 is given by:

$$\overrightarrow{F^1} = \iint\limits_{aper} \frac{\overrightarrow{M_e^1} e^{-jk|r-r'|}}{4\pi |r - r'|} ds' \tag{7}$$

From the identity [3]:

$$\frac{e^{-jk|r-r'|}}{|r - r'|} = \frac{1}{2\pi j} \int\limits_{-\infty}^{\infty} \int\limits_{-\infty}^{\infty} \frac{e^{j\{(x-x')k_x + (y-y')k_y - (z-z')k_z\}}}{k_z} dk_x dk_y \tag{8}$$

The electric and magnetic fields at any point in space are given by

$$\overrightarrow{E^1} = -\nabla \times \overrightarrow{F^1} \tag{9}$$

$$\overrightarrow{H^1} = -\frac{\nabla \times \overrightarrow{E^1}}{j\omega\mu} = \frac{1}{jk\eta}\nabla \times \nabla \times \overrightarrow{F^1} \tag{10}$$

From Equations (2) through (10), the externally scattered magnetic field at the plane of the aperture 1 ($z = 0$) is obtained as:

$$\overrightarrow{H}^{ext1} = \frac{1}{2\pi k\eta}\int_{-\infty}^{\infty}\int_{-\infty}^{\infty} k \times k \times \overrightarrow{\varepsilon}_s \times \frac{\widehat{u}_z}{k_z} e^{j(k_x x + k_y y)} dk_x dk_y$$

where $\overrightarrow{\varepsilon_s^1}$ is the Fourier Transform of the aperture electric field $\overrightarrow{E_s^1}$; it is given by

$$\overrightarrow{\varepsilon_s^1} = \widehat{u}_x \varepsilon_x^1 + \widehat{u}_y \varepsilon_y^1 = \frac{1}{2\pi}\iint_{Aperture} E_s^1(x', y', 0) e^{-j(k_x x' + k_y y')} dx' dy' \tag{11}$$

Therefore, the x-component of the magnetic field is given by

$$H_x^{ext1} = \frac{-1}{2\pi k\eta}\int_{-\infty}^{\infty}\int_{-\infty}^{\infty} \frac{k_x k_y \varepsilon_x^1 + \left(k^2 - k_x^2\right)\varepsilon_y^1}{k_z} e^{j(k_x x + k_y y)} dk_x dk_y \tag{12}$$

Substituting Equation (11) in (12) and simplifying, we obtain

$$H_x^{ext11} = -\frac{ab}{\pi^2 k\eta}\sum_{p=1}^{M} E_p^1 \int_{-\infty}^{\infty}\int_{-\infty}^{\infty} \frac{k^2 - k_x^2}{\left(k^2 - k_x^2 - k_y^2\right)^{1/2}} \mathrm{sinc}(k_y b) \frac{\left\{\begin{array}{ll} j\sin(k_x a) & \text{p even} \\ \cos(k_x a) & \text{p odd} \end{array}\right\}}{\frac{p\pi}{2}\left\{1 - \left(\frac{2ak_x}{p\pi}\right)^2\right\}} e^{j(k_x x + k_y y)} dk_x dk_y \tag{13}$$

Equation (13) gives the x-component of the externally scattered magnetic field at the aperture 1 due to the magnetic current source at the aperture 1. Similarly, the externally scattered magnetic field at the plane of the aperture 2 due to the magnetic current source at the

aperture 2 is obtained as:

$$H_x^{ext22} = -\frac{ab}{\pi^2 k\eta}\sum_{p=1}^{M} E_p^2 \int_{-\infty}^{\infty}\int_{-\infty}^{\infty} \frac{k^2-k_x^2}{\left(k^2-k_x^2-k_y^2\right)^{1/2}}\mathrm{sinc}(k_y b) \frac{\left\{\begin{array}{ll} j\sin(k_x a) & \text{p even} \\ \cos(k_x a) & \text{p odd}\end{array}\right\}}{\frac{p\pi}{2}\left\{1-\left(\frac{2ak_x}{p\pi}\right)^2\right\}} e^{j(k_x x+k_y y)}dk_x dk_y \quad (14)$$

The internally scattered field at the waveguide aperture is obtained by using the modal expansion approach [3]. The x-component of the internally scattered magnetic fields at apertures 1 and 2 are obtained as:

$$H_x^{\text{int1}} = \sum_{p=1}^{M} E_p^1 Y_{p0}^e \sin\left\{\frac{m\pi}{2a}(x+a)\right\} \quad (15)$$

$$H_x^{\text{int2}} = \sum_{p=1}^{M} E_p^2 Y_{p0}^e \sin\left\{\frac{m\pi}{2a}(x+a)\right\} \quad (16)$$

The externally radiated x-component of the magnetic fields at the plane of the probe's aperture due to the radiating apertures 1 and 2 are obtained as:

$$H_x^{ext31} = -\frac{ab}{\pi^2 k\eta}\sum_{p=1}^{M} E_p^1 \int_{-\infty}^{\infty}\int_{-\infty}^{\infty} \frac{k^2-k_x^2}{\left(k^2-k_x^2-k_y^2\right)^{1/2}}\mathrm{sinc}(k_y b) \frac{\left\{\begin{array}{ll} j\sin(k_x a) & \text{p even} \\ \cos(k_x a) & \text{p odd}\end{array}\right\}}{\frac{p\pi}{2}\left\{1-\left(\frac{2ak_x}{p\pi}\right)^2\right\}} e^{j(k_x x+k_y y-k_z z)}dk_x dk_y \quad (17)$$

$$H_x^{ext32} = -\frac{ab}{\pi^2 k\eta}\sum_{p=1}^{M} E_p^2 \int_{-\infty}^{\infty}\int_{-\infty}^{\infty} \frac{k^2-k_x^2}{\left(k^2-k_x^2-k_y^2\right)^{1/2}}\mathrm{sinc}(k_y b) \frac{\left\{\begin{array}{ll} j\sin(k_x a) & \text{p even} \\ cos(k_x a) & \text{p odd}\end{array}\right\}}{\frac{p\pi}{2}\left\{1-\left(\frac{2ak_x}{p\pi}\right)^2\right\}} e^{j(k_x x+k_y y-k_z z)}dk_x dk_y \quad (18)$$

where superscript 3 indicates the probe aperture. The x-component of the magnetic field at the plane of the probe aperture scattered by the magnetic current on the probe is the same form as the Equation (13) (or (14)). In addition, the x-component of the magnetic fields, at the plane of the radiating waveguide apertures 1 and 2 scattered by the magnetic current on the probe are same form as Equations (17) and (18), respectively.

The boundary conditions are simultaneously imposed at the plane of the radiating waveguide apertures 1 and 2, and at the plane of the near-field probe's aperture. The boundary condition at the region of the waveguide aperture is the tangential component of the magnetic field both inside the waveguide and outside it should be identical.

At $z = 0$ plane, the x-component of the magnetic field at the plane of the radiating aperture 1 is given by:

$$2H_x^{inc1} + H_x^{int1} = H_x^{ext11} + H_x^{ext12} + H_x^{ext13} \tag{19}$$

The x-component of the magnetic field at the plane of the radiating aperture 2 is given by:

$$2H_x^{inc2} + H_x^{int2} = H_x^{ext22} + H_x^{ext21} + H_x^{ext23} \tag{20}$$

At $z = z_1$ plane, the x-component of the magnetic field at the plane of the measuring probe's aperture is given by:

$$H_x^{int3} = H_x^{ext33} + 2H_x^{ext31} + 2H_x^{ext32} \tag{21}$$

Since the field is described by M basis functions, M unknowns are to be determined from the boundary condition. The Galerkin's specialization of the method of moments is used to obtain M different equations from the boundary condition to enable the determination of the E_p. The weighting function w_q is selected to be of the same form as the basis function e_p. The integral Equations (19), (20) and (21) are then converted into matrix form as:

$$2\left[L^{inc1}\right] + \left[L^{int1}\right]\left[E_p^1\right] = \left[L^{ext11}\right]\left[E_p^1\right] + \left[L^{ext12}\right]\left[E_p^2\right] + \left[L^{ext13}\right]\left[E_p^3\right] \tag{22}$$

$$2\left[L^{inc2}\right] + \left[L^{int2}\right]\left[E_p^2\right] = \left[L^{ext22}\right]\left[E_p^2\right] + \left[L^{ext21}\right]\left[E_p^1\right] + \left[L^{ext23}\right]\left[E_p^3\right] \tag{23}$$

$$\left[L^{int3}\right]\left[E_p^3\right] = \left[L^{ext33}\right]\left[E_p^3\right] + \left[L^{ext31}\right]\left[E_p^1\right] + \left[L^{ext32}\right]\left[E_p^2\right] \tag{24}$$

where the superscripts 1, 2 and 3 indicate the radiating apertures 1, 2 and probe aperture 3 respectively. The moment elements are obtained

as:

$$\left[L^{inc1}\right] = L_q^{inc1} = \left\langle H_x^{inc1}, w_q^1 \right\rangle = \left\{ \begin{array}{ll} -2abY_0 & q=1 \\ 0 & \text{otherwise} \end{array} \right\} \tag{25}$$

$$\left[L^{int1}\right] = L_{q,p}^{int1} = \left\langle H_x^{int1}(e_p^1), w_q^1 \right\rangle = \left\{ \begin{array}{ll} 2abY_p^e & p=q=m \ \& \ n=0 \\ 0 & \text{otherwise} \end{array} \right\} \tag{26}$$

$$\begin{aligned} \left[L^{ext11}\right] &= L_{q,p}^{ext11} = \left\langle H_x^{ext11}(e_p^1), w_q^1 \right\rangle \\ &= \frac{-4a^2b^2}{\pi^2 k\eta} \int\limits_{-\infty}^{\infty}\int\limits_{-\infty}^{\infty} \frac{k^2-k_x^2}{\left(k^2-k_x^2-k_y^2\right)^{1/2}} \mathrm{sinc}^2\left(k_y b\right) \\ &\qquad \frac{\left\{ \begin{array}{ll} \sin^2\left(k_x a\right) & p,q \text{ both even} \\ \cos^2\left(k_x a\right) & p,q \text{ both odd} \\ 0 & \text{otherwise} \end{array} \right\}}{\frac{p\pi}{2}\left\{1-\left(\frac{2ak_x}{p\pi}\right)^2\right\}\frac{q\pi}{2}\left\{1-\left(\frac{2ak_x}{q\pi}\right)^2\right\}} dk_x dk_y \end{aligned} \tag{27}$$

$$\begin{aligned} \left[L^{ext12}\right] &= L_{q,p}^{ext12} = \left\langle H_x^{ext12}(e_p^2), w_q^1 \right\rangle \\ &= \frac{-4a^2b^2}{\pi^2 k\eta} \int\limits_{-\infty}^{\infty}\int\limits_{-\infty}^{\infty} \frac{k^2-k_x^2}{\left(k^2-k_x^2-k_y^2\right)^{1/2}} \mathrm{sinc}^2\left(k_y b\right) \\ &\qquad \frac{\left\{ \begin{array}{ll} \sin^2\left(k_x a\right) & p,q \text{ both even} \\ \cos^2\left(k_x a\right) & p,q \text{ both odd} \\ 0 & \text{otherwise} \end{array} \right\}}{\frac{p\pi}{2}\left\{1-\left(\frac{2ak_x}{p\pi}\right)^2\right\}\frac{q\pi}{2}\left\{1-\left(\frac{2ak_x}{q\pi}\right)^2\right\}} e^{-j(k_x x_1 + k_y y_1)} dk_x dk_y \end{aligned} \tag{28}$$

$$\begin{aligned} \left[L^{ext13}\right] &= L_{q,p}^{ext13} = \left\langle H_x^{ext13}(e_p^3), w_q^1 \right\rangle \\ &= \frac{-4a^2b^2}{\pi^2 k\eta} \int\limits_{-\infty}^{\infty}\int\limits_{-\infty}^{\infty} \frac{k^2-k_x^2}{\left(k^2-k_x^2-k_y^2\right)^{1/2}} \mathrm{sinc}^2\left(k_y b\right) \end{aligned}$$

$$\frac{\left\{\begin{matrix}\sin^2(k_x a) & p,q \text{ both even}\\ \cos^2(k_x a) & p,q \text{ both odd}\\ 0 & \text{otherwise}\end{matrix}\right\}}{\frac{p\pi}{2}\left\{1-\left(\frac{2ak_x}{p\pi}\right)^2\right\}\frac{q\pi}{2}\left\{1-\left(\frac{2ak_x}{q\pi}\right)^2\right\}} e^{-j(k_x x_1+k_y y_1+k_z z_1)}dk_x dk_y \tag{29}$$

The expressions for $\left[L^{inc2}\right]$ is the same form as Equation (25), $\left[L^{int2}\right]$ and $\left[L^{int3}\right]$ are the same form as Equation (26), $\left[L^{ext22}\right]$ and $\left[L^{ext33}\right]$ are the same form as Equation (27), $\left[L^{ext21}\right]$ is the same as Equations (28) and $\left[L^{ext23}\right]$,$\left[L^{ext31}\right]$ and $\left[L^{ext32}\right]$ are the same form as Equation (29). Solving Equations (22), (23) and (24) simultaneously, we obtain the coefficients of the basis functions E_p^1, E_p^2 and E_p^3. From these coefficients, radiating element reflection coefficient and power received by the probe and hence the voltage are determined. The expression for power coupled into the probe waveguide in the TE_{10} mode is given by [4]:

$$P = 2abY_0 E_p^3 E_p^{3*} \tag{30}$$

Since measuring devices viz. spectrum analyzer has an input impedance of 50 ohms, the voltage is given by:

$$V = \sqrt{50 \times P}\,\text{volts} \tag{31}$$

3. RESULTS AND DISCUSSION

The standard X-band WR-90 rectangular waveguide in an infinite ground plane is used as a radiating element of the array radiator. The near-field measuring probe is also the same structure as the radiating element. Figure 2 shows the variation of the probe voltage with position of the probe, when the probe scan in the transverse (planar) plane and separation between radiating elements d is 2.54 cm (1 inch). It is evident from the plots that as the scan plane is closer to the radiator, probe voltage is larger. The variation of the probe voltage as a function of frequency, when the probe position is fixed at 1.5 cm, 3.0 cm and 5.0 cm in z-axis is shown in Figure 3. The measured results, when the probe is fixed at 5.0 cm from the radiator, are compared to the MoM results. Good agreement is obtained. Figure 4 shows the absolute reflection coefficient of the radiating element as the function of frequency, when the probe position is fixed in the near-field and

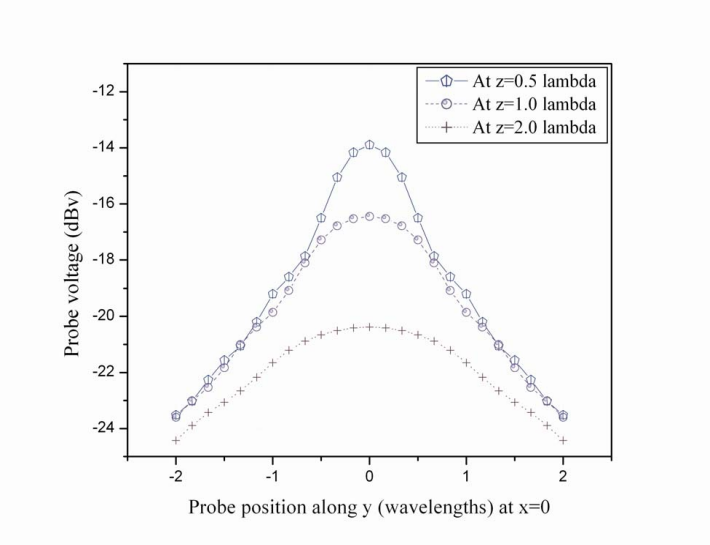

Figure 2. Probe voltage in x-y plane at $x = 0$ and $z = 0.5\lambda/1.0\lambda/2.0\lambda$, and at 10 GHz, when separation between radiating elements is $d = 2.54$ cm.

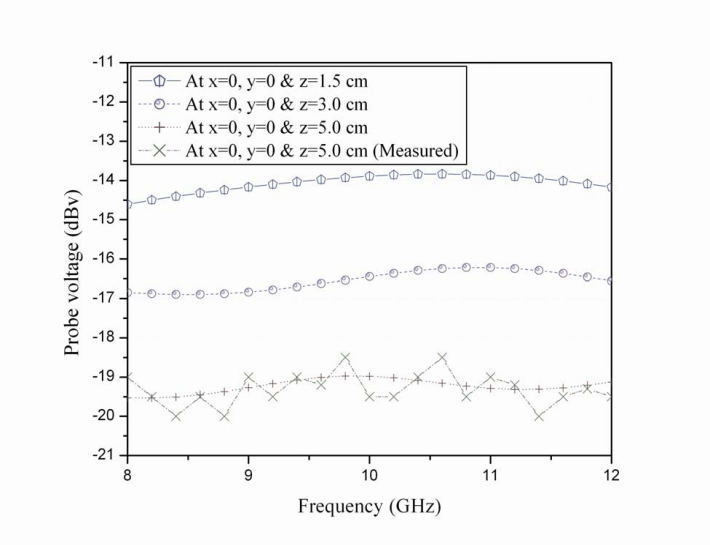

Figure 3. Probe voltage at $x = 0$, $y = 0$ and $z = 1.5$ cm/3.0 cm/5.0 cm, and compared to the measured results when the probe at $z = 5.0$ cm, over 8 to 12 GHz, when the separation between radiating elements is $d = 2.54$ cm.

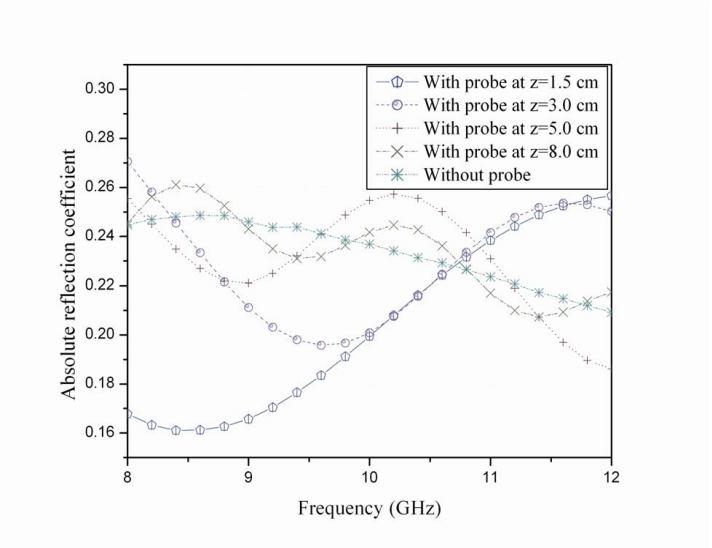

Figure 4. Absolute reflection coefficient for the radiating array element in the presence of the probe at $x = 0$, $y = 0$ and $z = 1.5\,\text{cm}/3.0\,\text{cm}/5.0\,\text{cm}/8.0\,\text{cm}$, and in the absence of the probe over 8 to 12 GHz when the separation between radiating elements is $d = 2.54\,\text{cm}$.

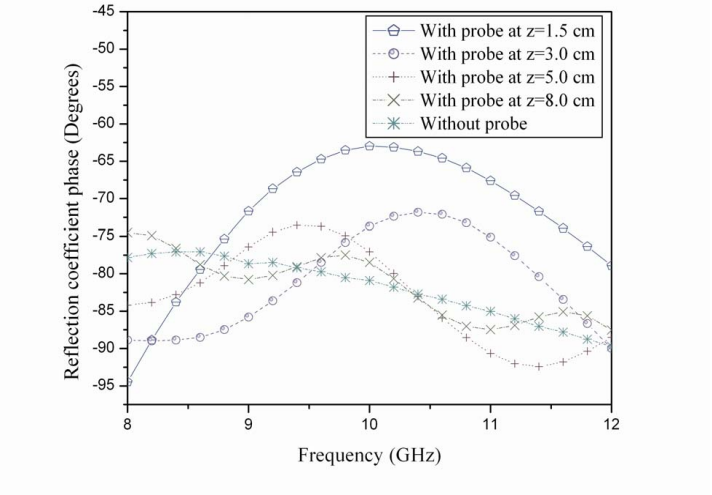

Figure 5. Reflection coefficient phase for the radiating array element in the presence of the probe at $x = 0$, $y = 0$ and $z = 1.5\,\text{cm}/3.0\,\text{cm}/5.0\,\text{cm}/8.0\,\text{cm}$, and in the absence of the probe over 8 to 12 GHz when the separation between radiating elements is $d = 2.54\,\text{cm}$.

separation between radiating elements d is 2.54 cm. When the probe is closer to the radiator, the reflection coefficient reduces, as it makes the better matching between radiator and probe. These are compared with the reflection coefficient of the radiating elements when there is no probe at the near-field. The reflection coefficient phase plots are shown in Figure 5.

4. CONCLUSION

When the radiating elements and probe are open-ended waveguides, because of multiple reflections and mutual coupling effect, and equivalent circuit properties of dominant mode the radiating element reflection coefficient improves. When the distance between probe and radiator reduces, the reflection coefficient decreases drastically, and the probe voltage increases, as evident from the plots. When the distance between the radiator and probe is larger, then the reflection coefficient values tend to the results obtained when there is no probe at the near-field.

REFERENCES

1. Harrington, R. F., *Field Computation by Moment Method*, Roger E. Krieger Publishing Company, USA, 1968.
2. Paramesha, S. and A. Chakrabarty, "Moment method analysis of rectangular waveguide as near-field measuring probe," *Microwave and Optical Technology Letters*, Vol. 48, No. 9, September 2006.
3. Harrington, R. F., *Time-Harmonic Electromagnetic Fields*, McGraw-Hill, New York, 1961.
4. Subrata, G., "Electromagnetic field estimation in aperture and slot antennas with their equivalent network representation," Ph.D. Dissertation, Department of E&ECE, IIT, Kharagpur, India, 1996.